

Parameters estimation from the diffusion MRI signal using a macroscopic model

This content has been downloaded from IOPscience. Please scroll down to see the full text.

2014 J. Phys.: Conf. Ser. 490 012117

(<http://iopscience.iop.org/1742-6596/490/1/012117>)

View [the table of contents for this issue](#), or go to the [journal homepage](#) for more

Download details:

IP Address: 5.51.13.66

This content was downloaded on 21/05/2014 at 10:12

Please note that [terms and conditions apply](#).

Parameters estimation from the diffusion MRI signal using a macroscopic model

¹H. T. Nguyen, ²J. R. Li, ³D. S. Grebenkov, ¹D. Le Bihan, ¹C. Poupon

¹ Neurospin - CEA Saclay, Gif-sur-Yvette, France

² INRIA Saclay-Equipe DEFI, CMAP, Ecole Polytechnique, Palaiseau, France

³ LPMC, CNRS – Ecole Polytechnique, Palaiseau, France

E-mail: hang.tuan.nguyen@cmap.polytechnique.fr, jingrebecca.li@inria.fr

Abstract. Diffusion magnetic resonance imaging (dMRI) probes the diffusion characteristics of a sample via the application of magnetic field gradient pulses. The dMRI signal from a heterogeneous sample includes the water proton magnetization from all spatial positions in a voxel. If the voxel consists of different diffusion compartments with weak exchange, while the duration of the diffusion-encoding gradient pulses is short compared to the diffusion time (the narrow pulse approximation), the dMRI signal can be approximated by the Karger model. A new macroscopic ODE model for the dMRI signal was recently derived mathematically from the microscopic multiple compartments Bloch-Torrey partial differential equation (PDE) without the narrow pulse restriction. We illustrate by numerical simulations that this ODE model accurately approximates the dMRI signal in a domain containing spherical cells of various sizes, and show preliminary results on solving the inverse problem to estimate the cellular volume fraction and surface area.

1. Introduction

A microscopic model for the diffusion magnetic resonance imaging (dMRI) signal is the Bloch-Torrey partial differential equation (PDE) [1, 2] on multiple compartments [3]. In general, for tissue geometries containing cells with permeable membranes, analytical solutions of this PDE are not known even for domains containing simple-shaped cells. One needs thus to resort to numerical simulations as well as to macroscopic models. An existing macroscopic model is the Karger model [4] which consists of a system of ordinary differential equations (ODEs) and takes into account a certain form of exchange between compartments. The validity of the Karger model and the “physical” meaning of the various parameters of this model was discussed in [5]. One important limitation of the Karger model is that the duration of the diffusion-encoding gradient pulses must be short compared to the diffusion time (the narrow-pulse approximation, see [6]). Here



we conduct a numerical study of a recently formulated macroscopic ODE model [7] that overcomes this limitation, in a 3D geometry containing spheres of various sizes, and solve the inverse problem to identify unknown parameters of the ODE model.

2. Microscopic multiple compartments Bloch-Torrey PDE

The starting point of the macroscopic model is the microscopic multiple compartment Bloch-Torrey PDE, which is a generalization of the original Bloch-Torrey PDE [1] to heterogeneous media. Inside a representative volume C , we define many spherical compartments, Ω^{sj} , $j = 1, \dots, P$, where each Ω^{sj} is a sphere. The complementary set, $\Omega^e = C \setminus \left(\bigcup_j \Omega^{sj}\right)$, is an extracellular compartment. For the macroscopic model to be discussed later, one can also group all cells of a certain type into a single compartment. The complex transverse water proton magnetization $M^l(\mathbf{r}, t|\mathbf{g})$ in each compartment Ω^l satisfies the Bloch-Torrey PDE [1]:

$$\frac{\partial M^l(\mathbf{r}, t|\mathbf{g})}{\partial t} = -If(t)(\gamma\mathbf{g} \cdot \mathbf{r}) M^l(\mathbf{r}, t|\mathbf{g}) + \nabla \cdot (D^0 \nabla M^l(\mathbf{r}, t|\mathbf{g})), \quad \forall l, \quad (1)$$

where we denote the amplitude and direction of the diffusion-encoding gradient by $\mathbf{g} = (g_1, g_2, g_3)$ (normalized direction $\mathbf{q} = \mathbf{g}/|\mathbf{g}|$) and its time profile by $f(t)$, I the imaginary unit, $\gamma = 2.67513 \times 10^8 \text{ rad s}^{-1} \text{ T}^{-1}$ the gyromagnetic ratio of the water proton, and D^0 the intrinsic water diffusion coefficient. For the pulsed gradient spin echo (PGSE) sequence [8], with two rectangular pulses of duration δ , separated by a time interval $\Delta - \delta$, the profile $f(t)$ is

$$f(t) = \begin{cases} 1, & 0 \leq t \leq \delta, \\ -1, & \Delta < t \leq \Delta + \delta, \\ 0, & \text{otherwise,} \end{cases} \quad (2)$$

where the starting time of the first gradient pulse is $t = 0$ and $\Delta > TE/2$.

We supplement the PDE in (1) with interface conditions at the interface Γ^{ln} where two compartments Ω^l and Ω^n come in contact. One interface condition is the continuity of flux:

$$D^0 \left(\nabla M^l(\mathbf{a}, t|\mathbf{g}) \cdot \mathbf{n}^l(\mathbf{a}) \right) = -D^0 \left(\nabla M^n(\mathbf{a}, t|\mathbf{g}) \cdot \mathbf{n}^n(\mathbf{a}) \right), \quad \mathbf{a} \in \Gamma^{ln}, \quad (3)$$

where $\mathbf{n}^l(\mathbf{a})$ and $\mathbf{n}^n(\mathbf{a})$ are the *outward*-point normals to Ω^l and Ω^n at \mathbf{a} , so in fact $\mathbf{n}^l(\mathbf{a}) = -\mathbf{n}^n(\mathbf{a})$. The second interface condition

$$D^0 \left(\nabla M^l(\mathbf{a}, t|\mathbf{g}) \cdot \mathbf{n}^l(\mathbf{a}) \right) = \kappa \left(M^n(\mathbf{a}, t|\mathbf{g}) - M^l(\mathbf{a}, t|\mathbf{g}) \right), \quad \mathbf{a} \in \Gamma^{ln}. \quad (4)$$

incorporates a permeability coefficient κ across Γ^{ln} . Finally, if the excitation of the magnetization in the imaging voxel is uniform, the following initial condition is added: $M(\mathbf{r}, 0|\mathbf{g}) = 1$, $\mathbf{r} \in \Omega^l$, $\forall l$. Then, same as [9], we assume that the computational domain $C = [-L_1/2, L_1/2] \times [-L_2/2, L_2/2] \times [-L_3/2, L_3/2]$ is extended by periodic copies

of itself. The dMRI signal measured in experiments (without the imaging gradients and T_2 effects) is proportional to

$$S_{PDE}(b) := \sum_l \int_{\mathbf{r} \in \Omega^l} M^l(\mathbf{r}, TE | \mathbf{g}) d\mathbf{r}, \quad (5)$$

where the b -value is defined as $b(\mathbf{g}) = \gamma^2 |\mathbf{g}^2| \delta^2 (\Delta - \delta/3)$. In a homogeneous medium, the signal attenuation is $\exp(-D^0 b)$.

3. Macroscopic ODE model

By an asymptotic analysis of the cell membrane permeability coefficient κ , a macroscopic (homogenized) model for the multiple compartment Bloch-Torrey PDE was obtained in [7], consisting of a system of ODEs:

$$\frac{dS_{ODE}^m(b, t)}{dt} = - \left(c(t) \gamma^2 \mathbf{g}^T \overline{D}^m \mathbf{g} + \sum_{l=1, l \neq m}^P \frac{1}{\tau_{ODE}^{lm}} \right) S_{ODE}^m(b, t) + \sum_{l=1, l \neq m}^P \frac{1}{\tau_{ODE}^{ml}} S_{ODE}^l(b, t) \quad m = 1, \dots, P$$

where

$$\frac{1}{\tau_{ODE}^{ml}} := \kappa \frac{|\Gamma^{ml}|}{|\Omega^l|} \implies \frac{\tau_{ODE}^{lm}}{\tau_{ODE}^{ml}} = \frac{|\Omega^m|}{|\Omega^l|} = \frac{v^m}{v^l}, \quad (6)$$

and $|\Gamma^{ml}|$ is the surface area of the interface between Ω^m and Ω^l ; $|\Omega^l|$ and v^l are respectively the volume and volume fraction of compartment Ω^l ($\sum_{l=1}^P v^l = 1$). For the pulsed gradient spin echo (PGSE) sequence, it was shown in [7]:

$$c(t) = \begin{cases} t^2, & 0 \leq t \leq \delta, \\ \delta^2, & \delta < t \leq \Delta, \\ (t - \Delta - \delta)^2, & \Delta < t \leq \Delta + \delta. \end{cases} \quad (7)$$

In the narrow pulse regime, $\delta \ll \Delta$, the ODE model reduces to the Karger model [4]:

$$\frac{dS_{KAR}^m(b, t)}{dt} = - \left(\delta^2 \gamma^2 \mathbf{g}^T \overline{D}^m \mathbf{g} + \sum_{l=1, l \neq m}^P \frac{1}{\tau^{lm}} \right) S_{KAR}^m(b, t) + \sum_{l=1, l \neq m}^P \frac{1}{\tau^{ml}} S_{KAR}^l(b, t) \quad m = 1, \dots, P.$$

Both the new ODE model and the Karger model rely on a system of coupled ODEs, subject to initial conditions: $S^l(b, 0) = v^l$, $l = 1, \dots, P$. The total dMRI signals for the ODE model and the Karger model are

$$S_{ODE}(b) = \sum_{m=1}^P S_{ODE}^m(b, TE), \quad S_{KAR}(b) = \sum_{m=1}^P S_{KAR}^m(b, TE). \quad (8)$$

The effective diffusion tensors, \overline{D}^m , $m = 1, \dots, P$, in the compartments can be obtained after solving three steady-state Laplace PDEs (see [7] for details).

4. Numerical results

We solved the multiple compartment Bloch-Torrey PDE in the computational domain $C = [-5\mu\text{m}, 5\mu\text{m}]^3$ containing the cellular configuration shown in Fig. 1a, with 76 spherical cells of radii in the range $0.6 - 2.55\mu\text{m}$, using the finite elements method described in [10]. We set the intrinsic diffusion coefficient in all the compartments to $D^0 = 3 \times 10^{-3}\text{mm}^2/\text{s}$. To obtain the ODE and the Karger model signals we combined the 76 spheres to form one compartment Ω^s . The extra-cellular space forms a second compartment Ω^e . The corresponding volume fractions are $v^s = 0.65$ and $v^e = 0.35$. The surface of the spherical compartment is $|\Gamma^{es}| = 1198\mu\text{m}^2$. The effective diffusion coefficient of Ω^s is $\bar{D}^s = 0$ because the spheres are compact. We computed the effective diffusion tensor of Ω^e (see [7] for details) to be $\bar{D}^e = \text{diag}(2.20, 2.25, 2.24) \times 10^{-3}\text{mm}^2/\text{s}$. For simplicity, we set $TE = \delta + \Delta$. The ODE signal is numerically solved by the Matlab routine *ode45* with absolute tolerance of 10^{-8} . The Karger solution is obtained explicitly by the eigen-decomposition of a 2×2 matrix [4].

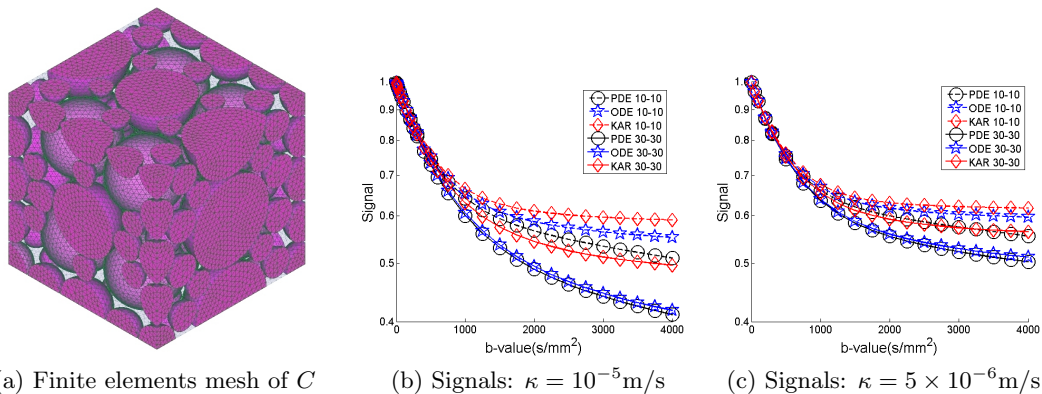


Figure 1: a) Finite element mesh of a domain $C = [-5\mu\text{m}, 5\mu\text{m}]^3$ containing spheres of many sizes. b) and c) DMRI signals with the PGSE sequence in the direction $\mathbf{g} = (1, 0, 0)$ at two diffusion times, $\delta = \Delta = 10\text{ms}$ and $\delta = \Delta = 30\text{ms}$, and two permeabilities $\kappa = 10^{-5}\text{m/s}$ and $\kappa = 5 \times 10^{-6}\text{m/s}$.

Figure 1b, 1c shows the dMRI signals at 20 b -values between 0 and $4000\text{s}/\text{mm}^2$ for two PGSE sequences, in the gradient direction $\mathbf{g} = (1, 0, 0)$. The signals are labeled: “PDE” (the multiple compartment Bloch-Torrey PDE), “ODE” and “KAR”, respectively. We can see that the ODE signal is significantly closer to the PDE signal than the Karger signal in these “non-narrow pulse” examples (δ is not small compared to Δ). We also see that the ODE signal is closer to the PDE signal as diffusion time increases. Both the ODE model and the Karger model operate with an “effective diffusion coefficient” (the slope of the logarithm of the signal versus the b -value) that is independent of the diffusion time. Thus, if the diffusion time is not long enough to get the “effective diffusion coefficient” independent of the diffusion time, then the ODE and the Karger models will definitely not be good approximations to the full PDE model. Note that this necessary condition is not sufficient to guarantee that the macroscopic models are accurate. We see that the slope of the logarithm of the signal curve is the same at $\delta = \Delta = 10\text{ms}$

and at $\delta = \Delta = 30\text{ms}$, but the ODE signal does not give a very good approximation to the PDE signal at the $\delta = \Delta = 10\text{ms}$, but it give an excellent approximation at $\delta = \Delta = 30\text{ms}$.

Now we consider the ‘‘PDE’’ signals in Fig. 1b and Fig. 1c as data (without noise) and solve the parameters estimation problem with the ODE and Karger models, i.e., determine the parameters of the macroscopic models from the signal. In particular, we assume that the volume of the computational domain $|C|$ and the permeability κ are known, and the effective diffusion tensor of the spherical compartment \overline{D}^s is set at 0. Thus, we consider three unknown parameters: 1) the effective extra-cellular diffusion coefficient $\mathbf{q}^T \overline{D}^e \mathbf{q}$, 2) the volume fraction of spherical compartment v^s , and 3) the surface area $|\Gamma^{es}|$. The Matlab routine *lsqnonlin* (tolerance of 10^{-8}) was used to find the least-square fit of the ‘‘PDE’’ signal to the ODE and the Karger models. The initial guess of $\mathbf{q}^T \overline{D}^e \mathbf{q}$ is $D^0/2$, of v^s is 0.5 and of $|\Gamma^{es}|$ is a random number in $[0.1, 10]$ times the true value. Using the parameters found by the Matlab routine, we computed the resulting $S_{ODE}(b_i)$ and $S_{KAR}(b_i)$ at the same 20 b-values shown in Fig. 1b and Fig. 1c. From these values we define the fitting error for each model in the following way:

$$E_{ODE}^{fit} \equiv \sqrt{\frac{1}{n_b} \sum_{i=1}^{n_b} \left| \frac{S_{PDE}(b_i) - S_{ODE}(b_i)}{S_{PDE}(b_i)} \right|^2}, \quad E_{KAR}^{fit} \equiv \sqrt{\frac{1}{n_b} \sum_{i=1}^{n_b} \left| \frac{S_{PDE}(b_i) - S_{KAR}(b_i)}{S_{PDE}(b_i)} \right|^2},$$

where n_b is the number of b-values ($n_b = 20$ in our example). The above expressions give a measure of the average relative error of the signal fit at all the b-values. Table 1 contains parameters estimation results for two membrane permeabilities, $\kappa = 10^{-5}\text{m/s}$ and $\kappa = 5 \times 10^{-6}\text{m/s}$, and at two diffusion times, $\delta = \Delta = 10\text{ms}$ and $\delta = \Delta = 30\text{ms}$; the table also includes the fitting errors.

We see that the estimation of all three parameters is better using the ODE model than the Karger model in these ‘‘non-narrow pulse’’ cases. In addition, because both macroscopic models are better approximations of the PDE model at the longer diffusion time ($\delta = \Delta = 30\text{ms}$) than the shorter diffusion time ($\delta = \Delta = 10\text{ms}$), the parameters estimation is also more accurate at the higher diffusion time for these examples.

5. Conclusion

We illustrated by numerical simulations that a recently formulated ODE model for the dMRI signal accurately approximates the dMRI signal from the full PDE model, and strongly outperforms the Karger model when the duration of the magnetic field gradient pulses is not small compared to the diffusion time. We estimated macroscopic geometrical quantities using the full PDE signal as the data without noise, and showed that the parameters estimation results using the new ODE model are promising. Future work on macroscopic parameter estimation in more physically realistic settings is in progress.

References

- [1] H. Torrey, ‘‘Bloch equations with diffusion terms,’’ *Physical Review Online Archive (Prola)*, vol. 104, no. 3, pp. 563–565, 1956.

$\kappa = 1 \times 10^{-5} \text{m/s}$		$\kappa = 5 \times 10^{-6} \text{m/s}$	
$\delta = \Delta = 10 \text{ms}$	$\delta = \Delta = 30 \text{ms}$	$\delta = \Delta = 10 \text{ms}$	$\delta = \Delta = 30 \text{ms}$
ODE (Karger)	ODE (Karger)	ODE (Karger)	ODE (Karger)
$E_{ODE}^{fit} \left(E_{KAR}^{fit} \right)$			
0.2% (0.3%)	0.03% (0.1%)	0.2% (0.3%)	0.04% (0.1%)
v^s (true value = 0.65)			
0.70 (0.73)	0.65 (0.72)	0.70 (0.73)	0.66 (0.70)
$ \Gamma^{es} $ (μm^2) (true value = 1198)			
2200 (4467)	1234 (2554)	3130 (6623)	1397 (2792)
$\mathbf{q}^T \overline{D^e} \mathbf{q}$ (mm^2/s) (true value = 0.0022)			
0.0026 (0.0030)	0.0023 (0.0028)	0.0026 (0.0030)	0.0023 (0.0026)

Table 1: Parameter estimation results for the domain in Fig. 1a. In each entry, the result is shown for the ODE model first, followed by the value for the Karger model in the parentheses.

- [2] W. S. Price, A. V. Barzykin, K. Hayamizu, and M. Tachiyu, "A model for diffusive transport through a spherical interface probed by pulsed-field gradient nmr," *Biophysical Journal*, vol. 74, pp. 2259–2271, May 1998.
- [3] D. S. Grebenkov, "Pulsed-gradient spin-echo monitoring of restricted diffusion in multilayered structures," *Journal of Magnetic Resonance*, vol. 205, pp. 181–195, Aug. 2010.
- [4] J. Karger, H. Pfeifer, and W. Heinik, "Principles and application of self-diffusion measurements by nuclear magnetic resonance," *Advances in magnetic resonance*, vol. 12, pp. 1–89, 1988.
- [5] E. Fieremans, D. S. Novikov, J. H. Jensen, and J. A. Helpert, "Monte carlo study of a two-compartment exchange model of diffusion," *NMR in Biomedicine*, vol. 23, no. 7, pp. 711–724, 2010.
- [6] D. Grebenkov, "Nmr survey of reflected brownian motion," *Reviews of Modern Physics*, vol. 79, no. 3, pp. 1077–1137, 2007.
- [7] J. Coatléven, H. Haddar, and J.-R. Li, "A new macroscopic model including membrane exchange for diffusion mri." See <http://www.cmap.polytechnique.fr/jingrebecali/preprints.html>, 2013.
- [8] E. O. Stejskal and J. E. Tanner, "Spin diffusion measurements: Spin echoes in the presence of a time-dependent field gradient," *The Journal of Chemical Physics*, vol. 42, no. 1, pp. 288–292, 1965.
- [9] J. Xu, M. Does, and J. Gore, "Numerical study of water diffusion in biological tissues using an improved finite difference method.," *Physics in medicine and biology*, vol. 52, p. N111, Apr. 2007.
- [10] D. V. Nguyen, D. Grebenkov, and J.-R. Li, "An efficient finite-elements code to simulate diffusion mri signals in complex tissue geometries." Submitted, see <http://www.cmap.polytechnique.fr/jingrebecali/preprints.html>, 2013.